High pressure shifts the β_1-adrenergic receptor to the active conformation in the absence of G protein

Layara Akemi Abiko, Anne Grahl, Stephan Grzesiek*

Focal Area Structural Biology and Biophysics, Biozentrum, University of Basel, CH-4056 Basel, Switzerland

*Address correspondence to:
Stephan Grzesiek
Focal Area Structural Biology and Biophysics, Biozentrum
University of Basel, CH-4056 Basel, Switzerland
Phone: ++41 61 267 2100
FAX: ++41 61 267 2109
Email: Stephan.Grzesiek@unibas.ch

Keywords: High-pressure; backbone NMR; G protein-coupled receptor; GPCR; void volume; conformational equilibrium; dynamics

ABSTRACT

G protein-coupled receptors (GPCRs) are versatile chemical sensors, which transmit the signal of an extracellular binding event across the plasma membrane to the intracellular side. This function is achieved via the modulation of highly dynamical equilibria of various conformational receptor states. Here we have probed the effect of pressure on the conformational equilibria of a functional thermostabilized β_1-adrenergic GPCR (β_1AR) by solution NMR. High pressure induces a large shift in the conformational equilibrium (midpoint ~600 bar) from the preactive conformation of agonist-bound β_1AR to the fully active conformation, which under normal pressure is only populated when a G protein or a G protein-mimicking nanobody (Nb) binds to the intracellular side of the β_1AR·agonist complex. No such large effects are observed for an antagonist-bound β_1AR or the ternary β_1AR·agonist·Nb80 complex. The detected structural changes of agonist-bound β_1AR around the orthosteric ligand binding pocket indicate that the fully active receptor occupies an ~100 $Å^3$ smaller volume than its preactive form. Most likely, this volume reduction is caused by the compression of empty (non-hydrated) cavities in the ligand binding pocket and the center of the receptor, which increases the ligand receptor interactions and explains the ~hundredfold affinity increase of agonists in the presence of G protein. The finding that isotropic pressure induces a directed motion from the preactive to the fully active GPCR conformation provides evidence of the high mechanical robustness of this important functional switch.

INTRODUCTION

G protein-coupled receptors (GPCRs) are important drug targets, which mediate the majority of cellular responses to a wide variety of extracellular stimuli across the membrane.[1] In recent years, a large number of crystal structures have provided detailed static pictures of diverse GPCRs in complex with many ligands.[2-8] Strikingly, the crystal structures of antagonist- or agonist-bound receptors are very similar (Figure 1A,B),[9] although their conformational states should encode their functional difference. Thus e.g. the RMSD of backbone and all heavy atoms positions between structures of the β_1-adrenergic receptor (β_1AR) in complex with an antagonist (Figure 1A) and an agonist (Figure 1B) are only 0.6 Å and 1.0 Å, respectively. Apparently more subtle differences such as changes of hydrogen bond patterns, individual sidechain contacts or conformational dynamics must be the cause of this functional difference. Substantial structural changes in crystal structures are only observed for ternary agonist·receptor complexes with a G protein or a G protein-mimicking nanobody bound to the intracellular effector side, in which transmembrane helices 5 and 6 (TM5,6) move by up to 14 Å outward from the transmembrane 7-helix bundle (Figure 1C),[10,11] corresponding for β_1AR to an RMSD relative to the agonist complex of 2.1 Å and 2.4 Å for backbone and all heavy atom positions, respectively.

Evidence from NMR, EPR, fluorescence and molecular dynamics simulations indeed indicates that the static pictures provided by crystallography are incomplete. Rather GPCRs are highly dynamic and sample several conformations in any particular functional state.[4,12-20] Notably agonist-bound receptors appear in a dynamical equilibrium between a preactive and a fully active state, where the latter is only populated when G proteins (or mimics) bind to the intracellular side.[14,17,21] Either one of these states may consist of an equilibrium of further conformational substates, which is modulated by particular ligand properties such as G protein efficacy, thereby determining the signaling level.[22] We denote in the following as fully active the conformation or state that is most compatible with the ternary agonist-G protein (or mimic) complex. The binding of the G protein effector to the preactive agonist complex also increases the agonist affinity by ~100 fold,[11,17,23,24] which is a hallmark of the allosteric coupling between the intracellular effector side and the extracellular orthosteric ligand binding pocket. It has been hypothesized that the affinity increase is due to the closing of a lid on top of the ligand binding pocket[25] or to a general reduction of the size of the ligand binding pocket.[26]

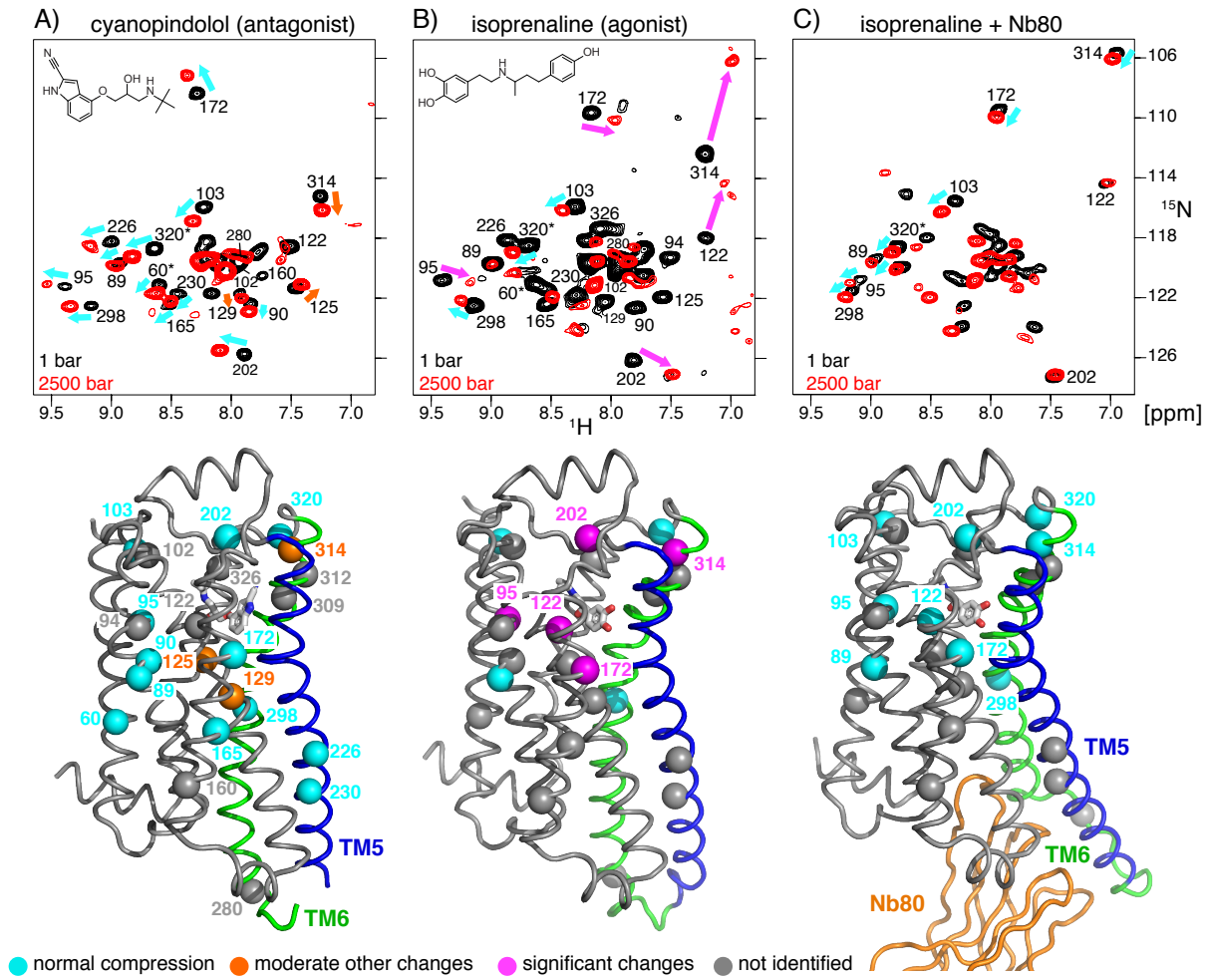

Figure 1. Pressure-dependent ^{1}H-^{15}N TROSY spectra (1 bar: black, 2500 bar: red) of ^{15}N-valine labeled β_1AR in complex with the antagonist cyanopindolol (A), the agonist isoprenaline (B), and in the ternary complex with isoprenaline and the G protein-mimicking Nb80 (C). Resonances are marked with assignment information (asterisks denote tentative assignments). Pressure-induced chemical shift changes of assigned residues are designated by colored arrows (cyan: normal hydrogen bond compression, orange: moderate other changes, magenta: significant changes). The respective residues are shown in the crystal structures of the corresponding β_1AR complexes (PDB codes 4bvn, 2y03 and 6h7j) as spheres with the same colors. Grey spheres represent unassigned residues.

We hypothesized that the variations in affinity between the different receptor states could involve different packing densities of the receptor-ligand interface and the interacting water. Thus the volume occupied by the GPCRs in their different functional states may be an essential thermodynamic quantity. The volume difference ΔV_{12} between two states 1 and 2 can be explored by the variation of pressure P, which to first order shifts their free energy difference $\Delta G_{12} = \Delta E_{12} + P\Delta V_{12} - T\Delta S_{12}$ (ΔE_{12} and ΔS_{12} are respective internal energy and entropy differences) and population ratio $w_1/w_2 = \exp(-\Delta G_{12}/kT)$, favoring the state with the smaller volume at higher pressure.[27] The population changes can be probed at atomic resolution by

NMR.[27-30] This has revealed details of pressure-induced protein unfolding[28-31] and local conformational equilibria at active sites of folded proteins.[32-37] However, so far no example of a pressure-induced global structural transition between two well-defined functional states of a folded protein has been reported.

Here we have investigated the conformational equilibria of the β_1-adrenergic receptor (β_1AR) in its principal functional states by solution NMR under the variation of pressure. We find that moderate pressure shifts the agonist-bound receptor from its preactive to the fully active conformation, which is normally reached only in the ternary agonist·G protein effector complex. Thus the fully active conformation of the agonist·GPCR complex including the interacting water is significantly more compact than the preactive conformation, providing a rationale for the increased agonist affinity and insights into the mechanism of allosteric transmembrane coupling in GPCRs.

RESULTS

Pressure induces the fully active conformation of agonist-bound β_1AR

Pressure-induced conformational changes of the β_1AR were followed by ^{1}H-^{15}N TROSY spectra (Figure 1) recorded on a detergent-solubilized ^{15}N-valine labeled, thermostabilized β_1AR mutant[17] in complexes with the antagonist cyanopindolol and the agonist isoprenaline, as well as in a ternary complex with isoprenaline and the G protein-mimicking nanobody 80 (Nb80).[10] This β_1AR mutant retains full functionality for agonist-induced G protein binding due to the reversion of two stabilizing mutations towards the native form (A227$^{5.58}$Y and L343$^{7.53}$Y, superscripts indicate Ballesteros-Weinstein numbering[38]). Of its total 28 valines, 19 have been assigned mainly by point mutations to ^{1}H-^{15}N resonances in the cyanopindolol, 20 in the isoprenaline, and 9 in the isoprenaline·Nb80 complex, respectively.[17]

For β_1AR in complex with the antagonist cyanopindolol, the ^{1}H-^{15}N chemical shift changes induced by the pressure increase from 1 to 2500 bar are very moderate (Figure 1A) with weighted average changes $\Delta\delta_{HN} < 0.2$ ppm (Figure S1) indicating only minor conformational changes. Almost all amide ^{1}H resonances, which could be followed unambiguously, experience downfield shifts (cyan arrows) as expected from the compression of the respective hydrogen bonds under pressure.[33] It is also noted that the linewidths of resonances are virtually unchanged between 1 and 2500 bar. Therefore the rotational correlation times are similar and major changes of the size and organization of the detergent micelle can be excluded.

In contrast to the antagonist complex, the pressure-induced chemical shift changes for the agonist isoprenaline complex are much more pronounced (Figure 1B, S1), whereas again linewidths are largely unchanged. In particular, valines located around the ligand binding pocket

(V95$^{2.57}$, V122$^{3.33}$, V172$^{4.56}$, V202^{ECL2}, V314$^{6.59}$) behave in an unusual way (magenta arrows): their amide ^{1}H chemical shifts move considerably upfield corresponding to an expansion of their H-bonds and also the ^{15}N shifts of residues V122$^{3.33}$, V202^{ECL2} and V314$^{6.59}$ change strongly, indicating a distortion of the backbone. Thus the ligand-binding pocket of the agonist complex is clearly much more compressible than for the antagonist complex.

Fewer assignments are available for the agonist isoprenaline·Nb80 complex in the fully active conformation. The assigned residues are mainly located at the extracellular face of the receptor (V103$^{2.65}$, V202^{ECL2}, V314$^{6.59}$, V320^{ECL3}) and around the ligand binding-pocket (V89$^{2.52}$, V95$^{2.57}$, V122$^{3.33}$, V172$^{4.56}$, V298$^{6.43}$). When the pressure is raised, their resonances change only very moderately and exhibit the usual amide ^{1}H downfield shift corresponding to H-bond compression (Figure 1C, cyan arrows). Hence similar to the antagonist complex, the ligand-binding pocket is not very compressible in the ternary complex. Unfortunately, no resonance assignments are available for valines at the intracellular side of this complex (Figure 1C gray spheres). However, since some of the unassigned resonances move noticeably under pressure in this complex, the intracellular side of the ternary complex appear more susceptible to pressure.

It is very striking to compare the spectra of agonist isoprenaline complex and the ternary agonist isoprenaline·Nb80 complex at 1 and 2500 bar (Figure 2). The spectra strongly differ at 1 bar corresponding to the difference of the preactive and the fully active conformations. However, at 2500 bar the spectra of both complexes are almost identical. In particular, all assigned resonances within the extracellular half of the agonist isoprenaline complex (V89$^{2.52}$, V95$^{2.57}$, V103$^{2.65}$, V122$^{3.33}$, V172$^{4.56}$, V202^{ECL2}, V314$^{6.59}$, V320^{ECL3}) fall exactly into the positions of the respective resonances of the ternary complex. Therefore under pressure, the entire exterior region of the agonist-bound receptor, including its ligand binding pocket, adopts the same fully active conformation as in the ternary complex. It is notable that also most (~13) of the remaining unassigned resonances are in very similar positions. Since many of these resonances are from residues within the intracellular half of the receptor, it can be concluded that also within this half of the receptor the conformations are similar. Therefore pressure alone can switch the preactive to the fully active conformation in most parts of the receptor even in the absence of the G protein mimic.

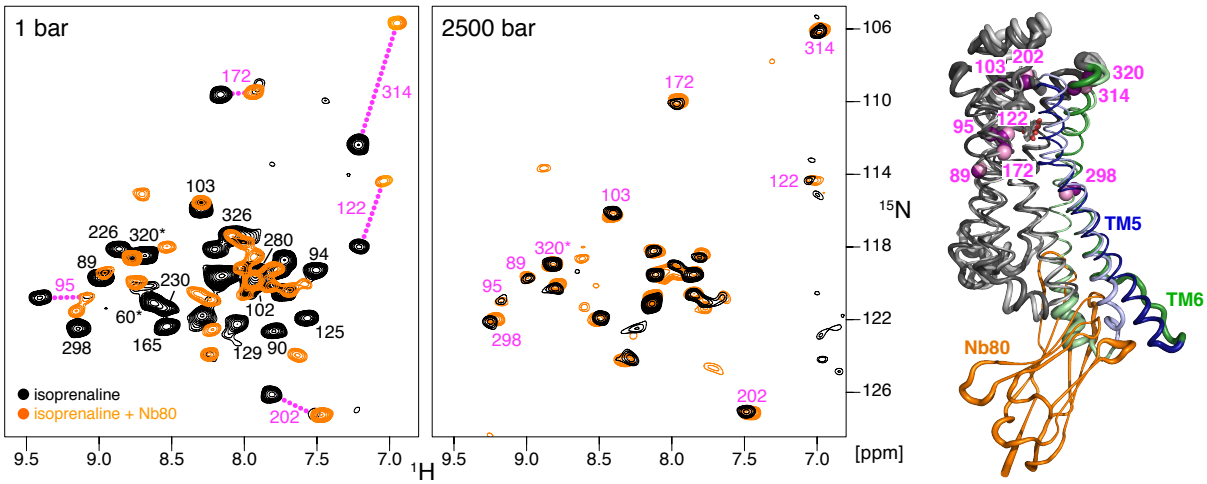

Figure 2. Comparison of isoprenaline·β_1AR (black) and isoprenaline·β_1AR·Nb80 (orange) ^{1}H-^{15}N TROSY spectra at 1 bar and 2500 bar. Resonances are marked with assignment information. Significant resonance shifts are highlighted by dashed magenta lines. Resonances that could be assigned at 2500 bar are indicated and represented as spheres in the crystal structures on the right: PDB 6h7j (active, dark colors) and PDB 2y03 (preactive, light colors).

Determination of volume difference ΔV_{fp} between fully active and preactive conformation

To determine the volume difference $\Delta V_{fp} = V_f - V_p$ between the fully active and the preactive conformation of the agonist isoprenaline complex, we followed its ^{1}H-^{15}N valine resonances continuously from 1 to 2500 bar (Figure 3, S2). Separate resonances visible for the two conformations at pressures from 1 to 900 bar show that these are in slow exchange on the chemical shift time scale with exchange times >~5 ms. Taking the intensity ratio of these resonances as a measure of the population ratio w_f/w_p, an approximately linear dependence of their free energy difference on the pressure is observed for the three well detectable residues V172$^{4.56}$, V202^{ECL2}, and V314$^{6.59}$ (Figure 3B). The linear fit provides an averaged free energy difference $\Delta G^0_{fp} = \Delta E_{fp} - T\Delta S_{fp}$ in the absence of pressure of 1.4 +/- 0.4 kT and an averaged volume difference ΔV_{fp} of -96 +/- 18 Å^3.

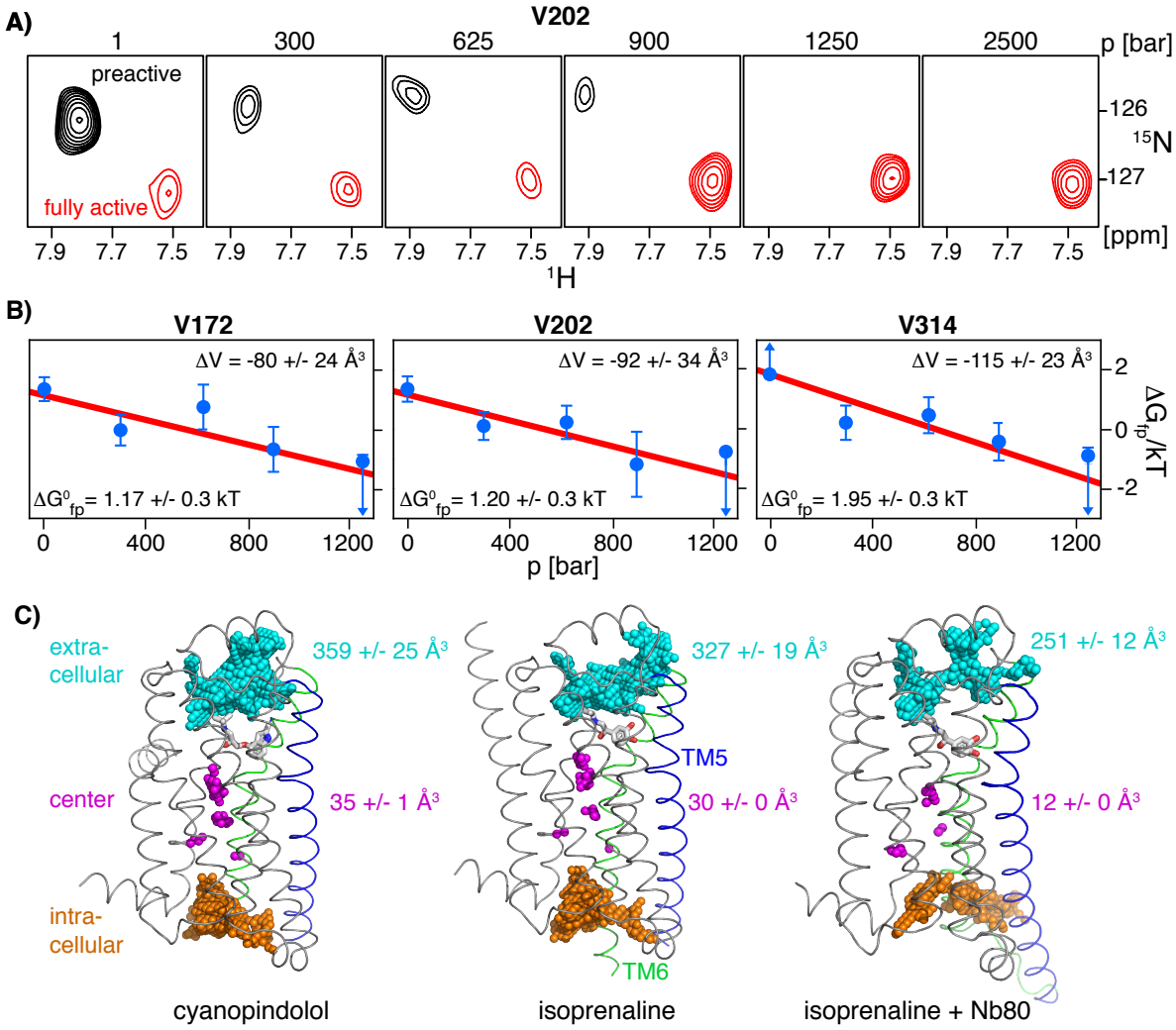

Figure 3. Quantitative analysis of the pressure-induced structural transition. A) Selected region of the ^{1}H-^{15}N TROSY spectra showing the resonance of V202^{ECL2} (located at the entrance of the orthosteric pocket) in the isoprenaline·β_1AR complex at different pressures. Black and red resonances correspond to the preactive and fully active state, respectively. Since the individual spectra were recorded on different samples, the total intensities of preactive and fully active state resonances are not identical across for the different pressure points. B) Free energy difference $\Delta G_{fp} = kT \cdot \ln(w_p/w_f) = \Delta G^0_{fp} + p\Delta V_{fp}$ derived from the resonance intensity ratios as a measure of the population ratios of the preactive and fully active state w_p/w_f for residues V172$^{4.56}$, V202^{ECL2}, and V314$^{6.59}$. Parameters $\Delta G^0_{fp} = \Delta E_{fp} - T\Delta S_{fp}$ and ΔV_{fp} obtained from a straight line fit are indicated. C) Structures of the β_1AR complex with antagonist cyanopindolol (2vt4), the agonist isoprenaline (2y03), and isoprenaline and Nb80 (6h7j) together with determined void volumes (shown as spheres, Table S1).

In principle, pressure-induced pH changes caused by the changes in hydration volume of buffer ions in their different ionization states may contribute to the observed conformational switch of the receptor. However, the pK of the used TRIS buffer has a very weak pressure dependence amounting to a pH change of only +0.12/kbar at pH 7.5.[39] Thus the pH of the β_1AR

solution increases maximally by 0.15 from 1 bar to 1250 bar. Such small changes are not expected to significantly change the populations of titratable groups within the β_1AR micelle. As a control we have also measured the spectra of β_1AR in complex with the agonist isoprenaline at pH 7.5 and 8.5 (Figure S3). The population of the fully active state as calculated from the average of V172, V202 and V314 intensities even decreases very slightly from 0.21 +/- 0.10 at pH 7.5 to 0.14 +/- 0.03 at pH 8.5. Therefore the slightly increased bulk pH can be safely excluded as the reason for the population increase of the fully active conformation from ~20 % at 1 bar to > ~83 % at 1250 bar indicated by Figure 3.

Possible causes of the pressure-induced transition and comparison to crystallographic voids

These results show that indeed the volume of the fully active state of the binary agonist isoprenaline·β_1AR complex including interacting water and detergent molecules is considerably smaller than that of the preactive state. Possible causes are a higher packing density of the receptor itself, of its internal or surface hydration (including interactions of charged groups), or of the surrounding detergent micelle, which we discuss in the following.

A priori, pressure effects on the organization of the detergent cannot be excluded since the molar reaction volume of micelle formation is relatively large (~28 Å^3 for decylmaltoside)[40] and pressure changes in particular the packing of the acyl chains.[41] However, since only the binary agonist complex, but not the antagonist complex nor the ternary agonist-Nb80 undergoes the pressure-induced transition, the receptor interior of the binary agonist complex must react differently to any such reorganization of the detergent and the resulting forces. Pressure-induced changes of charged groups within the receptor may also play a role, with histidines being the most likely candidates due to their pK in the neutral range. β_1AR contains only two histidines: H180$^{4.64}$ at the extracellular end of TM4 and H286$^{6.31}$ at the intracellular end of TM6. Both are oriented towards the water and are not expected to undergo significant changes related to receptor activation. Furthermore, the reaction volume for the histidine sidechain protonation is only -3.3 Å^3.[42,43] For these reasons, changes in the ionization states of histidines are unlikely to explain the observed β_1AR transition with a reaction volume of -96 Å^3.

In an effort to rationalize this reaction volume by variations in packing density within the various β_1AR complexes we analyzed the existing crystal structures for voids (Figure 3C, Table S1). While quantitative agreement of the crystallographic void volume differences to the measured reaction volume is not expected from such an analysis, since cryogenic cooling of crystals shrinks proteins and remodels the conformational distributions of protein side chains,[44] the analysis nevertheless revealed large rearrangements of the voids during function. Three

regions of voids can be distinguished: (i) the orthosteric binding pocket at the extracellular side, (ii) the center of the receptor below the orthosteric pocket, and (iii) the intracellular G protein binding pocket. All these functional sites of the receptor undergo significant structural changes during the transition from the preactive to the fully active state. The hydration state of the voids is largely unknown since only few tightly bound water molecules (4-6 for β_1AR) are observed in the crystal structures. However, both orthosteric and G protein binding pocket form large crevices accessible to water, and MD simulations indicate the presence of water molecules.[45,46]

The volume of the orthosteric ligand pocket shrinks from 327 Å^3 in the preactive to 251 Å^3 in the fully active conformation of the crystal structures. This reduction by 76 Å^3 can explain part of the pressure-derived volume difference ΔV_{fp} provided that a considerable part of the void in the preactive state is non-hydrated. Otherwise any filling water molecules would just move to the bulk in the active state, thereby occupying the same or an even larger volume (see below). Indeed, non-polar cavities smaller than ~80 Å^3 are predicted to be non-hydrated[47] and completely empty cavities larger than 100 Å^3 have been observed previously within proteins.[48,49] Therefore the possibility of a larger non-hydrated region within the orthosteric pocket of the preactive state should not be ruled out.

The central region of the receptor contains a number of smaller voids with a total volume of 30 Å^3 in the preactive state, which is reduced to 12 Å^3 in the fully active state. This is accompanied by a slight downward motion of the ligand isoprenaline by about 1-2 Å towards the center of the receptor (Figure 3C). Presumably these voids in the central region are much less accessible to water (no crystallographic water molecules are detected in these cavities) and contribute to the pressure effect.

In contrast to the orthosteric pocket, the intracellular G protein binding pocket widens in the fully active state (Figure 3C) to accommodate helix α5 of the G protein. A volume difference between these states cannot be determined reliably, since the pocket has a wide opening towards the intracellular space with no well-defined boundary for both the preactive and the fully active state. This makes it unlikely that large non-hydrated voids exist in this cavity in the preactive conformation, which could be compressed during the transition to the active conformation. Crystallographic observations of conserved water molecules in several GPCRs in combination with molecular dynamics simulations[45,46] indicate that the transition to the active state increases the hydration of this crevice. The exact hydration increase is unclear, since only few tightly bound water molecules are observable. This additional hydration may contribute to the observed volume reduction, because the average volume of a water molecule involved in protein hydration (22.9 Å^3 buried, 24.5 Å^3 surface water) as observed by crystallography[50] is smaller than the

volume of a bulk water molecule (29.7 Å^3). However, this reduction of the water volume is compensated to some extent by the larger volume of surface-exposed protein residues as compared to residues in the protein interior.[50] Therefore, if the volume change ΔV_{fp} resulted only from a transfer of bulk to hydration water, then the active receptor would have to coordinate at least 16 (≈96 Å^3/(29.7 Å^3 - 24 Å^3)) water molecules more than the preactive receptor. The observed hydration increase in recent MD simulations was significantly smaller.[46] As such, the effect from an increased hydration surface on the whole receptor and in particular within the G protein binding pocket is unlikely to explain the full extent of volume reduction in the active state.

Interestingly, the crystal structure of β_1AR in complex with the antagonist cyanopindolol has very similar void volumes as the agonist complex with isoprenaline (359 Å^3 orthosteric pocket, 35 Å^3 central region, Figure 3C, Table S1). The cyanopindolol complex does not show a pressure-induced structural transition to a compressed orthosteric pocket. Similar to many other antagonists, cyanopindolol has a larger head group than agonists such as isoprenaline. Apparently, the interactions of this larger head group with adjacent protein residues hinder the compression of the entire orthosteric pocket, thereby giving a mechanical rationale for the inhibitory function of antagonists with large head groups.

DISCUSSION

The higher compactness of the fully active state explains the affinity increase towards the agonist

The pressure-dependent equilibrium between preactive and fully active state has important implications for the thermodynamics of ligand binding and the underlying allosteric mechanisms. At normal pressure already 20 % of the orthosteric pocket is in the fully active state as evidenced from the V172$^{4.56}$, V202^{ECL2}, and V314$^{6.59}$ resonances (Figure 3). This indicates a conformational selection rather than an induced fit mechanism for this state, when the G protein (mimic) binds. We previously found that the pK for the agonist isoprenaline increases from 4.36 to 6.32 when Nb80 binds to the receptor in isolated insect cell membranes,[17] which is a highly characteristic feature of the allosteric coupling across the receptor. The higher compactness of the receptor in the fully active state and the concomitantly increased interactions between agonist and receptor provide a simple rationale for this affinity increase.

Pressure induces a directed motion of the receptor

It is astonishing that the application of pressure alone induces a well-defined transition from the preactive conformation of the agonist-bound receptor to a conformation that resembles the fully active ternary agonist·G protein mimic·receptor complex both in the vicinity of the

extracellular orthosteric pocket as well as (judged by the similarity of unassigned resonances) at its intracellular side. Thus a large part of the receptor undergoes this transition as a whole and not as individual unconnected parts. Instead of such a directed movement, one could rather have expected a non-directed random compression at several receptor sites leading to similar minor spectral changes as observed for the antagonist-bound receptor. The directed, pressure-induced transition indicates that the mechanical switch to the fully active conformation is very robust.

The reduction of a considerable void volume is an essential part of this mechanical switch. Albeit smaller volume reductions may come from the increased hydration of the G protein binding pocket, the largest reductions most likely stem from voids in the orthosteric pocket and the center of the preactive agonist-bound receptor. Some of these voids must be non-hydrated ('dry'), such that the transition to the fully active conformation reduces the volume. Hence this part of the structural transition will occur without entropic or enthalpic contributions from hydration as shown previously for a completely dry ligand binding pocket in thermolysin.[49] Indeed the free energy for hydrating such hydrophobic pockets is large enough to significantly destabilize proteins.[51] Dry pockets are very selective for hydrophobic interactions,[49] which would increase the mechanical robustness of the switch to the fully active state. The disappearance of voids in the center of the receptor below the ligand and the concomitant small motion of the ligand towards this center also provides a possible explanation for the pressure-induced directed motion: pressure compacts the orthosteric pocket and thereby pushes the ligand towards empty voids in the center of the receptor.

Conclusion

In summary we have shown that pressure induces a directed, functionally highly relevant transition from the preactive to the fully active conformation of a G protein binding-competent, thermostabilized β_1AR. This gives evidence of the mechanical robustness of this structural switch, which involves the filling of a considerable non-hydrated void volume. The specific nature of such dry voids as opposed to water-filled cavities may have important consequences for the functional interactions that drive the switch and may also offer possibilities for specific interventions via particularly strong hydrophobic interactions.[49] Currently experiments are ongoing to determine the exact nature of this void in the β_1AR. Very likely many functional transitions of other complex proteins are accompanied by sizeable volume changes, which can be studied at atomic resolution by pressure-dependent NMR spectroscopy.

Experimental Section

Sample Preparation

Expression of the ^{15}N-valine-labeled turkey β_1AR construct TS-β_1AR(A227Y/L343Y) in baculovirus-infected Sf9 cells, purification, assignments and binding of ligands and exchange between ligands were carried out as described previously.[17] The plasmid for Nb80 was a generous gift by Jan Steyaert and the Nb80 protein was purified according to the described procedure.[10]

NMR samples were prepared with typical receptor concentrations of 100-200 µM in 20 mM Tris-HCl, 100 mM NaCl, ~20 mM decylmaltoside (DM), 0.02 % NaN_3, 5 % D_2O (10 % for high-pressure experiments), pH 7.5 and 1 mM of cyanopindolol or 2 mM for isoprenaline solution, following a concentration step with a 50 kDa molecular weight cut-off centrifugal filter (Amicon) from ~15 µM receptor solubilized in 0.1 % DM. 20 mM sodium ascorbate was added to isoprenaline complex samples to prevent oxidation of the ligand. For formation of the ternary complex, a 1.2 molar equivalent of Nb80 was added to the isoprenaline·β_1AR complex.

NMR experiments

NMR experiments were performed on Bruker AVANCE 21.2 T (900 MHz) spectrometer equipped with a TCI cryoprobe at a temperature of 304 K. ^{1}H-^{15}N TROSY experiments were recorded as 80 (^{15}N) x 1024 (^{1}H) complex points and acquisition times of 16 ms (^{15}N) and 42 ms (^{1}H). For optimal sensitivity, the ^{1}H-^{15}N transfer time was reduced to 3.0 ms using a 1 s interscan delay. Typical total experimental times were 48 h. For high-sensitivity at 1 bar, measurements were performed with sample volumes of 250 µl in 5-mm diameter Shigemi tubes.

High-Pressure NMR experiments were carried out using a commercial high-pressure NMR cell (Daedalus Innovations LLC) with an inner diameter of 3 mm and an active volume of 120 µl. The tube was rated to 2,500 bar and used in an aluminium alloy static pressure cell connected to a high-pressure generator (High Pressure Equipment Company) via a pressure line. The line and the pressure generator were filled with extra low-viscosity paraffin wax (Sigma-Aldrich id 95369). Samples of 250 µl volume were placed in the high-pressure NMR tube, overlaid with paraffin wax and subsequently connected to the pressure line. ^{1}H-^{15}N TROSY experiments were recorded at 300, 625, 900, 1250 and 2500 bar for the isoprenaline complex and at 2500 bar for cyanopindolol and ternary complexes.

All NMR spectra were processed with NMRPipe[52] and evaluated with CcpNmr Analysis.[53] Referencing of the chemical shifts was obtained relative to the ^{1}H resonance of water and corrected for pressure and temperature effects as described previously.[30] Weighted ^{1}H-^{15}N chemical shift differences $\Delta\delta_{HN}$ were calculated as $\Delta\delta_{HN} = \sqrt{\left[(\Delta\delta H)^2 + \left(\frac{\Delta\delta N}{5}\right)^2\right]/2}$.

Analysis of crystal structures

RMSDs of atom positions between various β_1AR crystal structures were calculated comprising the 7 transmembrane helices and the extracellular loop 2 (ECL2), i.e. residues 39-65, 78-103, 113-140, 158-178, 188-193, 206-235, 283-313, 325-343.

Voids in the crystal structures were quantified using the program Hollow 1.2.[54] with a grid spacing of 1.0 Å and a sphere size of 4 Å for the definition of the outer receptor surface. Water, lipid molecules, and the G protein ligand mimic were removed before the analysis. Table S1 lists the detected void volumes in various crystal structures of β_1AR. Water and lipid molecules were removed before the void calculation.

Supporting Information

The Supporting Information is available free of charge on the ACS Publications website at DOI:XXX

Supplementary Figures S1-S2 showing further NMR evidence of the pressure dependence of β_1AR (PDF) and Table S1 listing calculated void volumes for various β_1AR crystal structures.

Acknowledgments

This work was supported by the Swiss National Science Foundation (grants 31-149927 and 31-173089 to S.G.) and by a Fellowship for Excellence by the Biozentrum Basel International PhD Program (to A.G.). We gratefully acknowledge Dr. Timothy Sharpe of the Biozentrum Biophysics facility for expert help with the biophysical characterization of β_1AR as well as Drs. Judith Habazettl, Hans-Jürgen Sass, Shin Isogai, Xavier Deupi, and Gebhard Schertler for helpful discussions.

References

(1) Alexander, S. P.; Christopoulos, A.; Davenport, A. P.; Kelly, E.; Marrion, N. V.; Peters, J. A.; Faccenda, E.; Harding, S. D.; Pawson, A. J.; Sharman, J. L.; Southan, C.; Davies, J. A. THE CONCISE GUIDE to PHARMACOLOGY 2017/18: G Protein-Coupled Receptors. *British Journal of Pharmacology* **2017**, *174*, S17–S129.

(2) Caffrey, M. A Comprehensive Review of the Lipid Cubic Phase or in Meso Method for Crystallizing Membrane and Soluble Proteins and Complexes. **2015**, *71* (1), 3–18.

(3) Grisshammer, R. New Approaches Towards the Understanding of Integral Membrane Proteins: a Structural Perspective on G Protein-Coupled Receptors. *Protein Sci* **2017**, *26* (8), 1493–1504.

(4) Manglik, A.; Kobilka, B. K.; Steyaert, J. Nanobodies to Study G Protein-Coupled Receptor Structure and Function. *Annu. Rev. Pharmacol. Toxicol.* **2017**, *57* (1), 19–37.

(5) Carpenter, B.; Tate, C. G. Active State Structures of G Protein-Coupled Receptors Highlight the Similarities and Differences in the G Protein and Arrestin Coupling Interfaces. *Curr. Opin. Struct. Biol.* **2017**, *45*, 124–132.

(6) de Graaf, C.; Song, G.; Cao, C.; Zhao, Q.; Wang, M.-W.; Wu, B.; Stevens, R. C. Extending the Structural View of Class B GPCRs. *Trends Biochem Sci* **2017**, *42* (12), 946–960.

(7) Smith, J. S.; Lefkowitz, R. J.; Rajagopal, S. Biased Signalling: From Simple Switches to Allosteric Microprocessors. *Nat Rev Drug Discov* **2018**, *268*, 4625.

(8) Hilger, D.; Masureel, M.; Kobilka, B. K. Structure and Dynamics of GPCR Signaling Complexes. *Nat. Struct. Mol. Biol.* **2018**, *25* (1), 4–12.

(9) Venkatakrishnan, A. J.; Deupi, X.; Lebon, G.; Tate, C. G.; Schertler, G. F.; Babu, M. M. Molecular Signatures of G-Protein-Coupled Receptors. *Nature* **2013**, *494* (7436), 185–194.

(10) Rasmussen, S. G. F.; Choi, H.-J.; Fung, J. J.; Pardon, E.; Casarosa, P.; Chae, P. S.; Devree, B. T.; Rosenbaum, D. M.; Thian, F. S.; Kobilka, T. S.; Schnapp, A.; Konetzki, I.; Sunahara, R. K.; Gellman, S. H.; Pautsch, A.; Steyaert, J.; Weis, W. I.; Kobilka, B. K. Structure of a Nanobody-Stabilized Active State of the B(2) Adrenoceptor. *Nature* **2011**, *469* (7329), 175–180.

(11) Carpenter, B.; Nehmé, R.; Warne, T.; Leslie, A. G. W.; Tate, C. G. Structure of the Adenosine A2A Receptor Bound to an Engineered G Protein. *Nature* **2016**, *536* (7614), 104–107.

(12) Liu, J. J.; Horst, R.; Katritch, V.; Stevens, R. C.; Wuthrich, K. Biased Signaling Pathways in B2-Adrenergic Receptor Characterized by 19F-NMR. *Science* **2012**, *335* (6072), 1106–1110.

(13) Kofuku, Y.; Ueda, T.; Okude, J.; Shiraishi, Y.; Kondo, K.; Maeda, M.; Tsujishita, H.; Shimada, I. Efficacy of the B2-Adrenergic Receptor Is Determined by Conformational Equilibrium in the Transmembrane Region. *Nat. Commun.* **2012**, *3*, 1045–1049.

(14) Nygaard, R.; Zou, Y.; Dror, R. O.; Mildorf, T. J.; Arlow, D. H.; Manglik, A.; Pan, A. C.; Liu, C. W.; Fung, J. J.; Bokoch, M. P.; Thian, F. S.; Kobilka, T. S.; Shaw, D. E.; Mueller, L.; Prosser, R. S.; Kobilka, B. K. The Dynamic Process of Beta(2)-Adrenergic Receptor Activation. *Cell* **2013**, *152* (3), 532–542.

(15) Manglik, A.; Kobilka, B. The Role of Protein Dynamics in GPCR Function: Insights From the β2AR and Rhodopsin. *Curr. Opin. Cell Biol.* **2014**, *27*, 136–143.

(16) Okude, J.; Ueda, T.; Kofuku, Y.; Sato, M.; Nobuyama, N.; Kondo, K.; Shiraishi, Y.; Mizumura, T.; Onishi, K.; Natsume, M.; Maeda, M.; Tsujishita, H.; Kuranaga, T.; Inoue, M.; Shimada, I. Identification of a Conformational Equilibrium That Determines the Efficacy and Functional Selectivity of the Mu-Opioid Receptor. *Angew Chem Int Ed Engl* **2015**, *54* (52), 15771–15776.

(17) Isogai, S.; Deupi, X.; Opitz, C.; Heydenreich, F. M.; Tsai, C.-J.; Brueckner, F.; Schertler, G. F. X.; Veprintsev, D. B.; Grzesiek, S. Backbone NMR Reveals Allosteric Signal Transduction Networks in the Beta1-Adrenergic Receptor. *Nature* **2016**, *530* (7589), 237–241.
(18) Ye, L.; Van Eps, N.; Zimmer, M.; Ernst, O. P.; Scott Prosser, R. Activation of the A2A Adenosine G-Protein-Coupled Receptor by Conformational Selection. *Nature* **2016**, *533* (7602), 265–268.
(19) Latorraca, N. R.; Venkatakrishnan, A. J.; Dror, R. O. GPCR Dynamics: Structures in Motion. *Chem Rev* **2016**, *117* (1), 139–155.
(20) Eddy, M. T.; Lee, M.-Y.; Gao, Z.-G.; White, K. L.; Didenko, T.; Horst, R.; Audet, M.; Stanczak, P.; McClary, K. M.; Han, G. W.; Jacobson, K. A.; Stevens, R. C.; Wuthrich, K. Allosteric Coupling of Drug Binding and Intracellular Signaling in the a 2A Adenosine Receptor. *Cell* **2017**.
(21) Manglik, A.; Kim, T. H.; Masureel, M.; Altenbach, C.; Yang, Z.; Hilger, D.; Lerch, M. T.; Kobilka, T. S.; Thian, F. S.; Hubbell, W. L.; Prosser, R. S.; Kobilka, B. K. Structural Insights Into the Dynamic Process of B2-Adrenergic Receptor Signaling. *Cell* **2015**, *161* (5), 1101–1111.
(22) Solt, A. S.; Bostock, M. J.; Shrestha, B.; Kumar, P.; Warne, T.; Tate, C. G.; Nietlispach, D. Insight Into Partial Agonism by Observing Multiple Equilibria for Ligand-Bound and G S -Mimetic Nanobody-Bound B 1 -Adrenergic Receptor. *Nat. Commun.* **2017**, *8* (1), 1795.
(23) Staus, D. P.; Strachan, R. T.; Manglik, A.; Pani, B.; Kahsai, A. W.; Kim, T. H.; Wingler, L. M.; Ahn, S.; Chatterjee, A.; Masoudi, A.; Kruse, A. C.; Pardon, E.; Steyaert, J.; Weis, W. I.; Prosser, R. S.; Kobilka, B. K.; Costa, T.; Lefkowitz, R. J. Allosteric Nanobodies Reveal the Dynamic Range and Diverse Mechanisms of G-Protein-Coupled Receptor Activation. *Nature* **2016**, *535* (7612), 448–452.
(24) Kruse, A. C.; Ring, A. M.; Manglik, A.; Hu, J.; Hu, K.; Eitel, K.; Hübner, H.; Pardon, E.; Valant, C.; Sexton, P. M.; Christopoulos, A.; Felder, C. C.; Gmeiner, P.; Steyaert, J.; Weis, W. I.; Garcia, K. C.; Wess, J.; Kobilka, B. K. Activation and Allosteric Modulation of a Muscarinic Acetylcholine Receptor. *Nature* **2013**, *504* (7478), 101–106.
(25) Rasmussen, S. G. F.; Edwald, E.; Manglik, A.; Du, Y.; Pardon, E.; Steyaert, J. Allosteric Coupling From G Protein to the Agonist-Binding Pocket in GPCRs. *Nature* **2016**, *535* (7610), 182–186.
(26) Warne, T.; Edwards, P. C.; Doré, A. S.; Leslie, A. G. W.; Tate, C. G. Molecular Basis for High-Affinity Agonist Binding in GPCRs. *Science* **2019**, *364* (6442), 775–778.
(27) Frauenfelder, H.; Alberding, N. A.; Ansari, A.; Braunstein, D.; Cowen, B. R.; Hong, M. K.; Iben, I. E. T.; Johnson, J. B.; Luck, S. Proteins and Pressure. *The Journal of Physical Chemistry* **1990**, *94* (3), 1024–1037.
(28) Kitahara, R.; Okuno, A.; Kato, M.; Taniguchi, Y.; Yokoyama, S.; Akasaka, K. Cold Denaturation of Ubiquitin at High Pressure. *Magn Reson Chem* **2006**, *44 Spec No*, S108–S113.
(29) Kremer, W.; Arnold, M.; Munte, C. E.; Hartl, R.; Erlach, M. B.; Koehler, J.; Meier, A.; Kalbitzer, H. R. Pulsed Pressure Perturbations, an Extra Dimension in NMR Spectroscopy of Proteins. *J. Am. Chem. Soc.* **2011**, *133* (34), 13646–13651.
(30) Vajpai, N.; Nisius, L.; Wiktor, M.; Grzesiek, S. High-Pressure NMR Reveals Close Similarity Between Cold and Alcohol Protein Denaturation in Ubiquitin. *Proc. Natl. Acad. Sci. USA* **2013**, *110* (5), E368–E376.
(31) Charlier, C.; Courtney, J. M.; Alderson, T. R.; Anfinrud, P.; Bax, A. Monitoring (15)N Chemical Shifts During Protein Folding by Pressure-Jump NMR. *J. Am. Chem. Soc.* **2018**, *140* (26), 8096–8099.

(32) Kitahara, R.; Sareth, S.; Yamada, H.; Ohmae, E.; Gekko, K.; Akasaka, K. High Pressure NMR Reveals Active-Site Hinge Motion of Folate-Bound Escherichia Coli Dihydrofolate Reductase. *Biochemistry* **2000**, *39* (42), 12789–12795.
(33) Nisius, L.; Grzesiek, S. Key Stabilizing Elements of Protein Structure Identified Through Pressure and Temperature Perturbation of Its Hydrogen Bond Network. *Nat Chem* **2012**, *4* (9), 711–717.
(34) Kalbitzer, H. R.; Rosnizeck, I. C.; Munte, C. E.; Narayanan, S. P.; Kropf, V.; Spoerner, M. Intrinsic Allosteric Inhibition of Signaling Proteins by Targeting Rare Interaction States Detected by High-Pressure NMR Spectroscopy. *Angew Chem Int Ed Engl* **2013**, *52* (52), 14242–14246.
(35) Munte, C. E.; Beck Erlach, M.; Kremer, W.; Koehler, J.; Kalbitzer, H. R. Distinct Conformational States of the Alzheimer Beta-Amyloid Peptide Can Be Detected by High-Pressure NMR Spectroscopy. *Angew Chem Int Ed Engl* **2013**, *52* (34), 8943–8947.
(36) Maeno, A.; Sindhikara, D.; Hirata, F.; Otten, R.; Dahlquist, F. W.; Yokoyama, S.; Akasaka, K.; Mulder, F. A. A.; Kitahara, R. Cavity as a Source of Conformational Fluctuation and High-Energy State: High-Pressure NMR Study of a Cavity-Enlarged Mutant of T4 Lysozyme. *Biophys. J.* **2015**, *108* (1), 133–145.
(37) Alderson, T. R.; Roche, J.; Gastall, H. Y.; Dias, D. M.; Pritisanac, I.; Ying, J.; Bax, A.; Benesch, J. L. P.; Baldwin, A. J. Local Unfolding of the HSP27 Monomer Regulates Chaperone Activity. *Nat. Commun.* **2019**, *10* (1), 1068.
(38) Ballesteros, J. A.; Weinstein, H. Integrated Methods for the Construction of Three-Dimensional Models and Computational Probing of Structure-Function Relations in G Protein-Coupled Receptors. *Methods in Neurosciences* **1995**, *25*, 366–428.
(39) Quinlan, R. J.; Reinhart, G. D. Baroresistant Buffer Mixtures for Biochemical Analyses. *Anal Biochem* **2005**, *341* (1), 69–76.
(40) Fan, H. Y.; Nazari, M.; Chowdhury, S.; Heerklotz, H. Volume and Expansivity Changes of Micelle Formation Measured by Pressure Perturbation Calorimetry. *Langmuir* **2011**, *27* (5), 1693–1699.
(41) Alvares, R.; Gupta, S.; Macdonald, P. M.; Prosser, R. S. Temperature and Pressure Based NMR Studies of Detergent Micelle Phase Equilibria. *J. Phys. Chem. B* **2014**, *118* (21), 5698–5706.
(42) Weber, H. H. Die Bjerrumsche Zwitterionentheorie Und Die Hydratation Der Eiweisskoerper. *Biochemische Zeitschrift* **1930**, *218*, 1–35.
(43) Hauer, J.; Müller, K.; Lüdemann, H. D.; Jaenicke, R. The Pressure Dependence of the Histidine Ring Protonation Constant Studied by 1H HR-NMR. *Febs Letters* **1981**, *135* (1), 135–138.
(44) Fraser, J. S.; van den Bedem, H.; Samelson, A. J.; Lang, P. T.; Holton, J. M.; Echols, N.; Alber, T. Accessing Protein Conformational Ensembles Using Room-Temperature X-Ray Crystallography. *Proc. Natl. Acad. Sci. USA* **2011**, *108* (39), 16247–16252.
(45) Yuan, S.; Filipek, S.; Palczewski, K.; Vogel, H. Activation of G-Protein-Coupled Receptors Correlates with the Formation of a Continuous Internal Water Pathway. *Nat. Commun.* **2014**, *5* (1), 11435.
(46) Venkatakrishnan, A. J.; Ma, A. K.; Fonseca, R.; Latorraca, N. R.; Kelly, B.; Betz, R. M.; Asawa, C.; Kobilka, B. K.; Dror, R. O. Diverse GPCRs Exhibit Conserved Water Networks for Stabilization and Activation. *Proc. Natl. Acad. Sci. USA* **2019**, *116* (8), 3288–3293.
(47) Yin, H.; Feng, G.; Clore, G. M.; Hummer, G.; Rasaiah, J. C. Water in the Polar and Nonpolar Cavities of the Protein Interleukin-1β †. *J. Phys. Chem. B* **2010**, *114* (49), 16290–16297.

(48) Qvist, J.; Davidovic, M.; Hamelberg, D.; Halle, B. A Dry Ligand-Binding Cavity in a Solvated Protein. *Proc. Natl. Acad. Sci. USA* **2008**, *105* (17), 6296–6301.
(49) Krimmer, S. G.; Cramer, J.; Schiebel, J.; Heine, A.; Klebe, G. How Nothing Boosts Affinity: Hydrophobic Ligand Binding to the Virtually Vacated S1′ Pocket of Thermolysin. *J. Am. Chem. Soc.* **2017**, *139* (30), 10419–10431.
(50) Gerstein, M.; Chothia, C. Packing at the Protein-Water Interface. *Proc. Natl. Acad. Sci. USA* **1996**, *93* (19), 10167–10172.
(51) Nucci, N. V.; Fuglestad, B.; Athanasoula, E. A.; Wand, A. J. Role of Cavities and Hydration in the Pressure Unfolding of T4 Lysozyme. *Proc. Natl. Acad. Sci. USA* **2014**, *111* (38), 13846–13851.
(52) Delaglio, F.; Grzesiek, S.; Vuister, G. W.; Zhu, G.; Pfeifer, J.; Bax, A. NMRPipe: a Multidimensional Spectral Processing System Based on UNIX Pipes. *J. Biomol. NMR* **1995**, *6* (3), 277–293.
(53) Vranken, W. F.; Boucher, W.; Stevens, T. J.; Fogh, R. H.; Pajon, A.; Llinas, M.; Ulrich, E. L.; Markley, J. L.; Ionides, J.; Laue, E. D. The CCPN Data Model for NMR Spectroscopy: Development of a Software Pipeline. *Proteins-Structure Function and Bioinformatics* **2005**, *59* (4), 687–696.
(54) Ho, B. K.; Gruswitz, F. HOLLOW: Generating Accurate Representations of Channel and Interior Surfaces in Molecular Structures. *BMC Struct Biol* **2008**, *8* (1), 49.